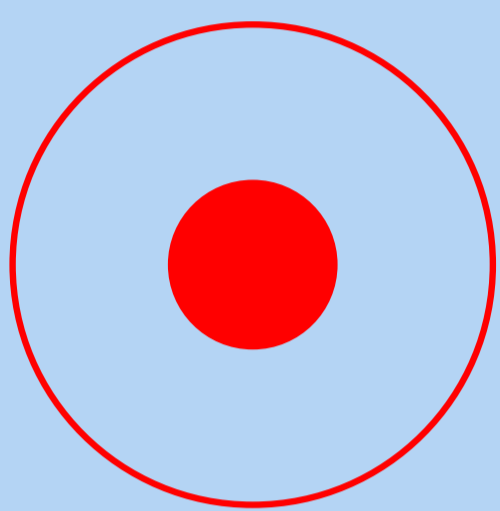


## Motivation

Molecular clouds show a hierarchy of complex structure which can be attributed to interstellar turbulence. To study the dynamic nature of molecular cloud turbulence we have to compare the statistical properties of molecular cloud observations with hydrodynamic and magnetohydrodynamic turbulence simulations. There is a large variety of statistical measures to characterise the scaling of the density and the velocity structure. We have tested these tools with respect to their sensitivity and applicability to molecular line data and turbulence models. The most significant measures are applied in the comparison of observational data with numerous turbulence models to reveal the dynamical state of the molecular clouds.

## The $\Delta$ -variance

The  $\Delta$ -variance (Stutzki et al. 1998) measures the relative structural variation on a certain scale. It can be used to determine the spatial scaling properties of arbitrary quantities, e.g. intensity maps or velocity centroid maps.



The  $\Delta$ -variance is computed by convolving the image with a "French hat" wavelet of varying diameter and measuring the variance of the resulting map.

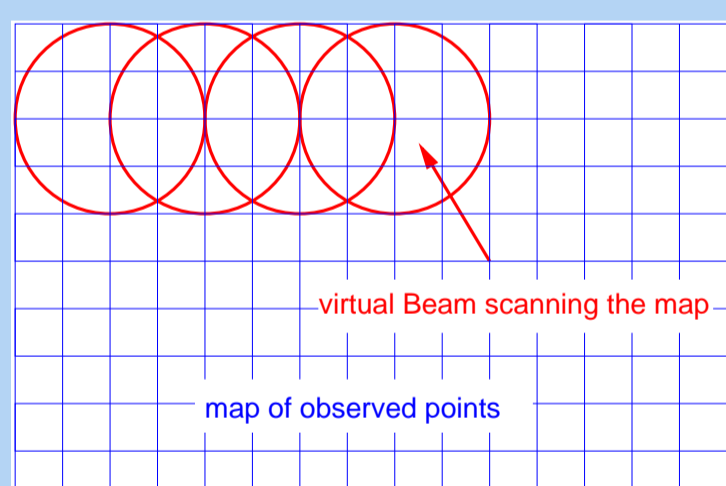
The slope  $\alpha$  of the  $\Delta$ -variance as a function of lag (filter size) is related to the spectral index  $\beta$  of the power spectrum of the image

$$P(|\vec{k}|) \propto |\vec{k}|^{-\beta} \quad \text{by} \quad \beta = \alpha + 2$$

The  $\Delta$ -variance measures the spectral index in a way which is more robust with respect to edge and gridding effects than the Fourier transform.

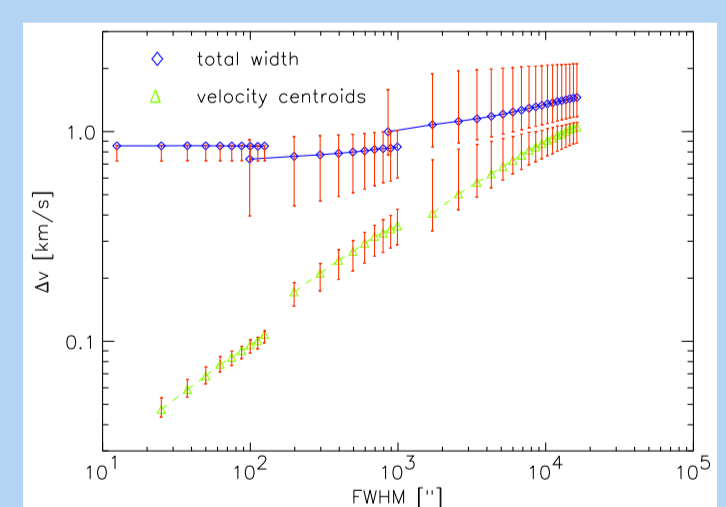
## The size-linewidth relation

The traditional size-linewidth relation (Goodman et al. 1998) relies on the selection of discrete objects (clumps or clouds) which are impossible to define in filamentary turbulent structures. We use a scanning-beam size-linewidth relation to trace different length scales.



The map is scanned by virtual telescope beams of varying size. We compute the average velocity variation measured within a beam depending on its size.

We consider either the total line width within the virtual beam tracing the full velocity distribution or the distribution of centroid velocities only. In the first case all components along a line of sight contribute. In the latter case only the lateral variation of the velocities is measured. Thus, the comparison of both functions can reveal the depth of the cloud along the line of sight.



Size-linewidth relations for the MCLD 123.5+24.9 data. The three maps provide the three connected size ranges.

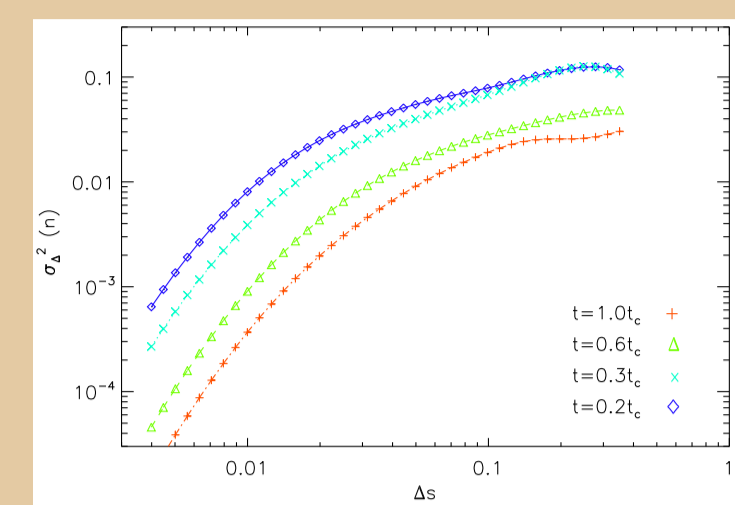
The size-linewidth relation for the centroid velocities can detect the spatial velocity drift on all scales. We find a **power law index of 0.5 covering all scales**. Comparing it with the relation for the total line profiles we estimate a cloud depth corresponding to about 150' or 6 pc respectively.

For most turbulence models the size-line width relation is close to a **power law with an exponent between 0.4 and 0.6** independent from the evolutionary state or the magnetic field. Above the driving scale we find a flattening of the relation that should be detectable in corresponding observational data.

## Turbulence simulations

Simulations of hydrodynamic or magnetohydrodynamic turbulence were performed using the ZEUS-3D code (Stone & Norman 1992) on grids of  $64^3 - 256^3$  zones. The simulated isothermal, supersonic turbulence is either continuously driven by Gaussian perturbations at chosen scales or decaying after an initial driving.

### $\Delta$ -variance of the column density

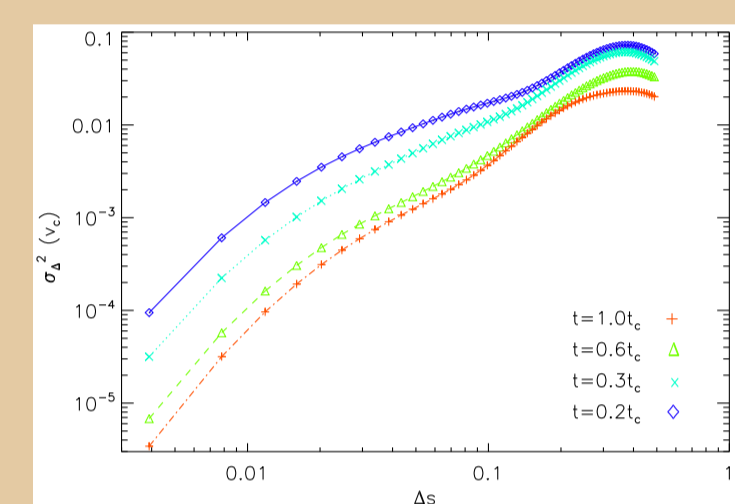


Time sequence of  $\Delta$ -variances for a model of decaying hydrodynamic turbulence where the energy was initially injected at the largest scale.

At the beginning of the simulation, the scale of the energy input appears as prominent peak in the  $\Delta$ -variance followed by an inertial power-law at smaller scales. At scales below five zones ( $\Delta s < 0.02$ ), structure is blurred by the artificial viscosity and numerical dissipation. The spectral index  $\beta$  varies between 2.4 to 2.7 in the inertial range and 4.0 at the dissipation scale.

During the decay of turbulence, structure is removed at the small-scale end by dissipation distorting the power-law behaviour and leading to an overall curved  $\Delta$ -variance plot.

### The centroid velocity maps

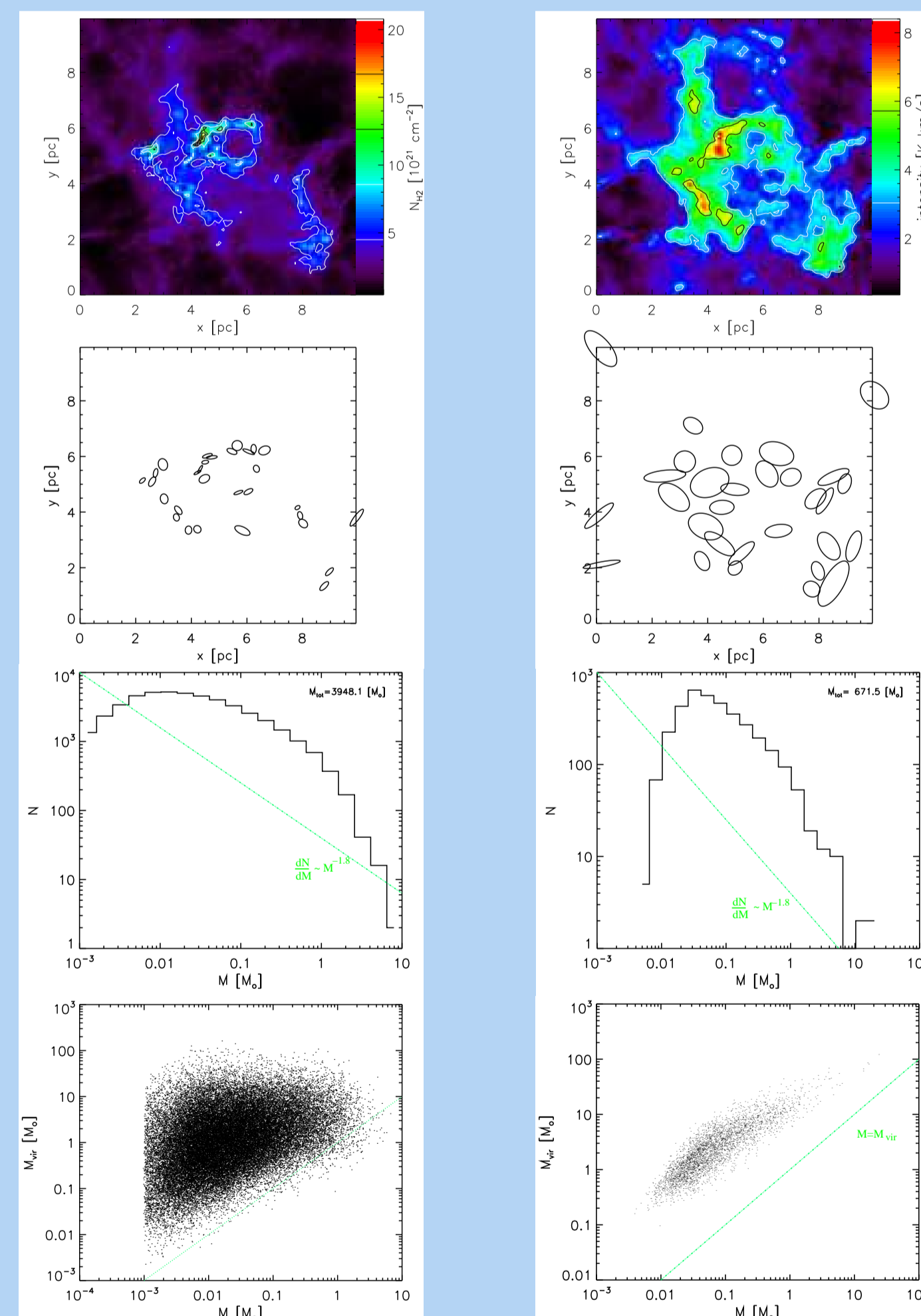


$\Delta$ -variance of the centroid velocity maps for the decaying hydrodynamic model shown above.

The velocity structure shows the same general behaviour as the density structure but the dissipation scale appears less pronounced. The spectral index  $\beta$  changes from 3.6 at large scales to 4.2 at the smallest scales.

## Clump decomposition

Molecular clouds are often characterised by their decomposition into clumps and the resulting clump properties. Using the turbulence models we compared the clumps detectable in corresponding molecular line data with the clumps present in the density structure.

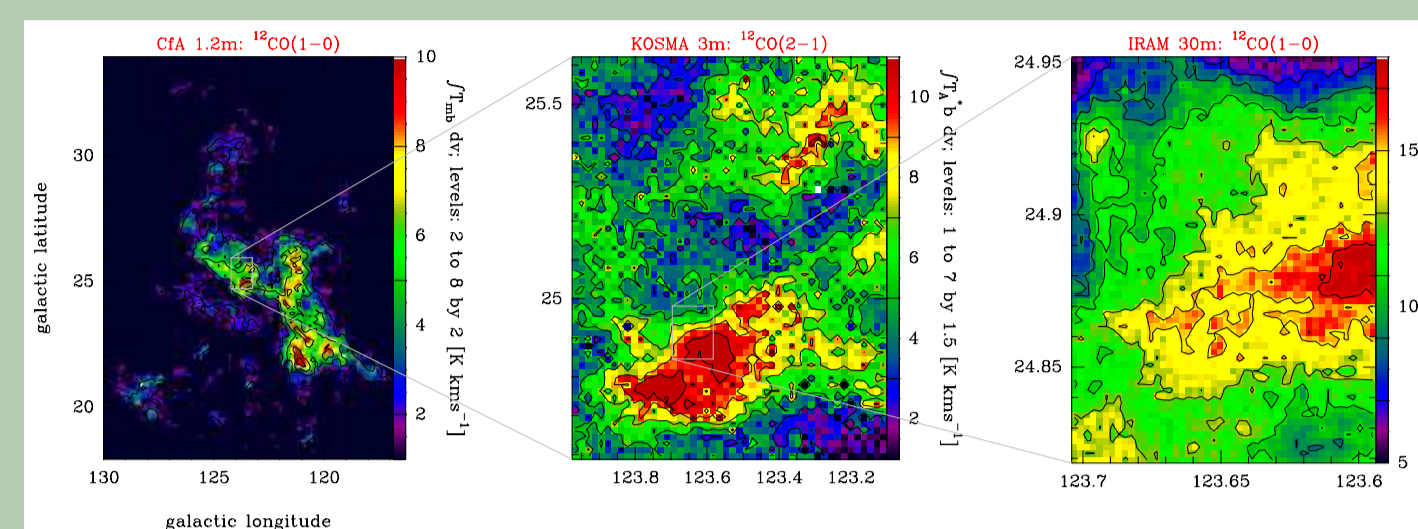


The left panels show the results of GAUSSCLUMPS applied to the density structure of a large-scale driven, not self-gravitating model. The right panels demonstrate the clump data obtained from a  $^{13}\text{CO}$  observation of the model cloud with  $S/N=100$ . Each row shows the integrated map, the location of the 30 most massive clumps, the clump mass spectrum, and the virial mass versus the integrated mass of each clump.

The observed **clump spectrum does not reflect the physical distribution** of clumps although it is determined by the model data. **Observational artifacts**, including radiative transfer effects, **produce a pseudo-virialisation** explaining the difference between observations and the results of Vázquez-Semadeni et al. (1997).

## Observational data

- We have analysed extended CO maps of various molecular cloud complexes with different star-formation activity.
- A preferred example is MCLD 123.5+24.9 in the Polaris Flare, a high latitude cloud without star formation, where we have a combined set of observations available, taken in various CO isotopes and with different resolutions providing a large dynamic range of spatial scales.



CO maps of three nested data cubes of MCLD 123.5+24.9 observed with the CFA 1.2m telescope (Heithausen & Thaddeus 1990), the KOSMA 3m telescope (Bensch et al. 2001), and the IRAM 30m telescope (Falgarone et al. 1998)

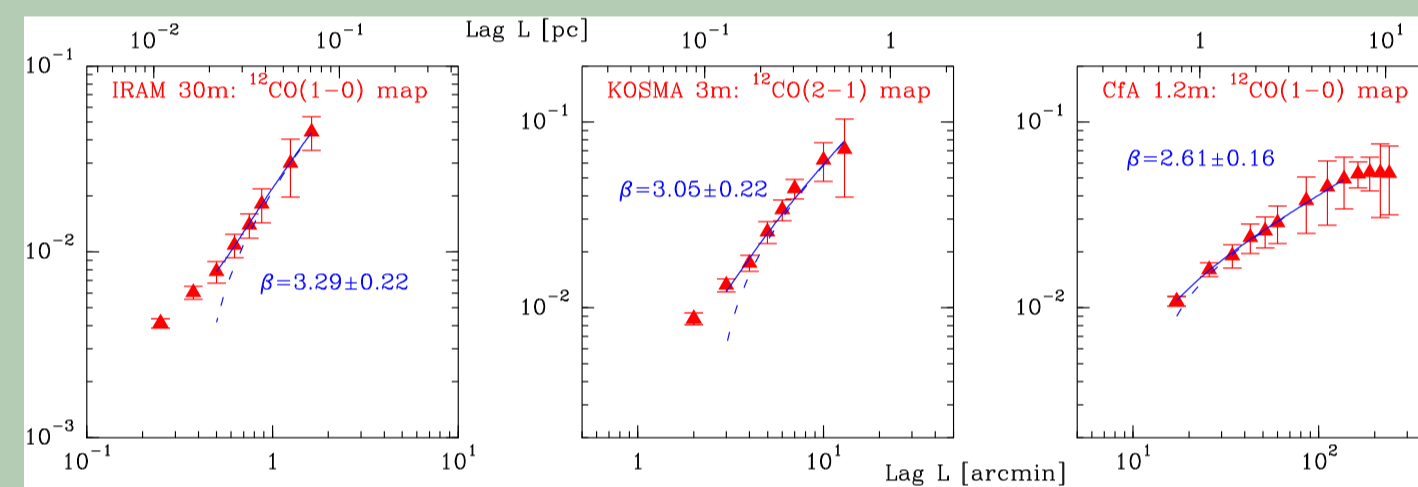
## The observed structure

### The intensity maps

Analysis of molecular cloud surveys taken with the Bell Labs 7 m telescope in  $^{13}\text{CO}$  1-0 (HPBW=100''):

source	distance [pc]	$\beta = \alpha + 2$	lag L [pc] ( $\Delta$ -var fit)
Orion A	450	$2.54 \pm 0.05$	0.39-7.50
Orion B	415	$2.68 \pm 0.12$	0.36-6.92
NGC 2264	800	$2.54 \pm 0.12$	0.93-7.14
Mon R2	950	$2.76 \pm 0.12$	0.69-2.16
NGC1333	350	$3.07 \pm 0.10$	0.31-2.52

Analysis of the MCLD 123.5+24.9 observations:



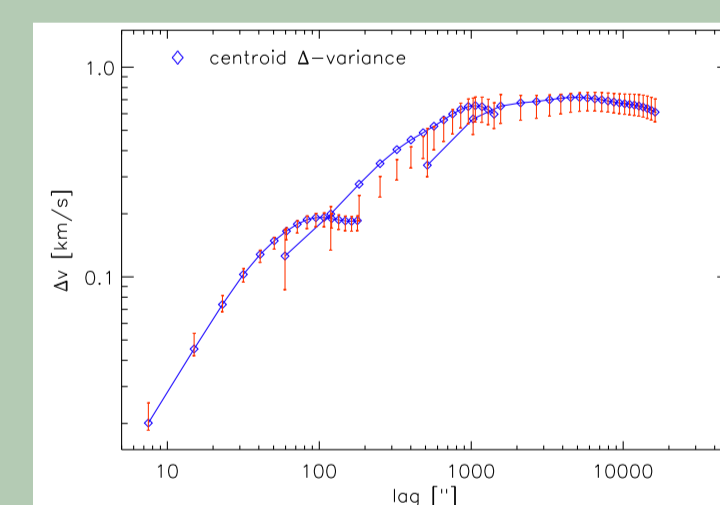
The  $\Delta$ -variance  $\sigma_{\Delta}^2$  of the three nested intensity maps. The spectral indices  $\beta$  correspond to the solid lines including corrections for noise and beam smearing

Summary of the MCLD observations (assumed distance 150 pc):

telescope	transition	telescope HPBW	$\beta = \alpha + 2$	lag L [pc] ( $\Delta$ -var fit)
CFA 1.2m	$^{12}\text{CO}1-0$	8.7'	$2.61 \pm 0.16$	0.75-6.0
KOSMA 3m	$^{12}\text{CO}2-1$	2.2'	$3.05 \pm 0.22$	0.13-0.6
FCRAO 14m	$^{13}\text{CO}1-0$	0.78'	$3.22 \pm 0.15$	0.06-0.48
IRAM 30m	$^{12}\text{CO}1-0$	0.35'	$3.29 \pm 0.22$	0.02-0.07
IRAM 30m	$^{12}\text{CO}2-1$	0.175'	$3.25 \pm 0.23$	0.02-0.07

On the scale of a typical map most observations are reasonably fitted by a power law. There is only one systematic trend visible: the spectral index  $\beta$  decreases when increasing the absolute length scales mapped.

### The velocity scaling



$\Delta$ -variance of the velocity centroids. Beyond 3000'' the centroid map is dominated by regions without measurable emission so that the values are not significant there.

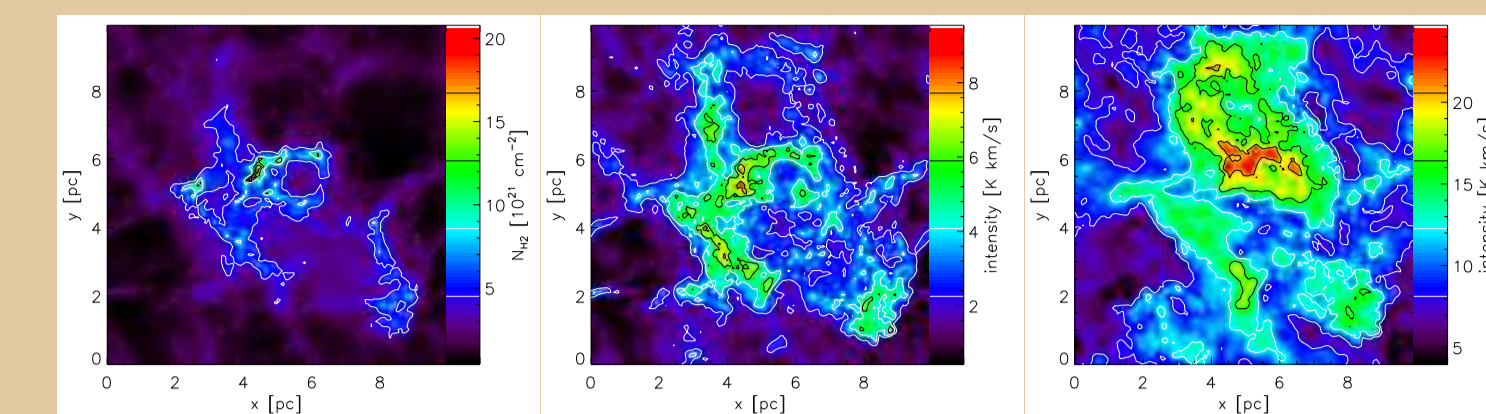
We find one smooth relation for the velocity drift connecting all three maps. The slope changes from 1.3 at the smallest scales to 0.9 at the end of the significant range.

### The general behaviour

- Using the nested maps in MCLD 123.5+24.9 the  $\Delta$ -variance shows a **significant deviation from self-similarity** both in the intensity and the velocity structure.
- The spectral index  $\beta$  changes from 2.6 to 3.3 in the **density structure** and from 3.9 to 4.3 in the **velocity structure** when going to the smallest scales.
- The dynamic range and resolution in the observations of the other molecular clouds is insufficient to detect such a change. They support, however, the general picture of a **structure scaling behaviour depending only on the absolute length scale**.

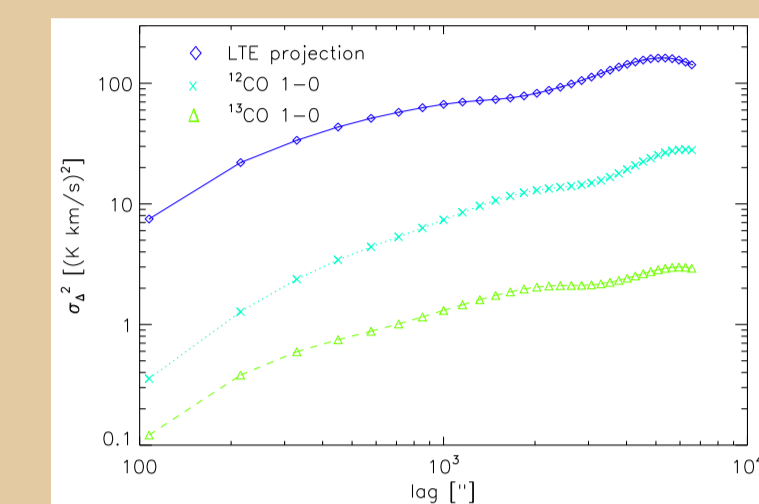
## Radiative transfer effects

We have computed the CO line intensity emerging from a model cloud in a two-scale approximation, assuming statistically large scale isotropy of the exciting radiation field.



Comparison of the projected density structure from a hydrodynamic model (left panel), with the structure appearing in  $^{13}\text{CO}$  1-0 (center panel) and in  $^{12}\text{CO}$  1-0 (right panel).

The molecular line radiative transfer "hides" all material outside of a certain density range either by under-excitation or by saturation.

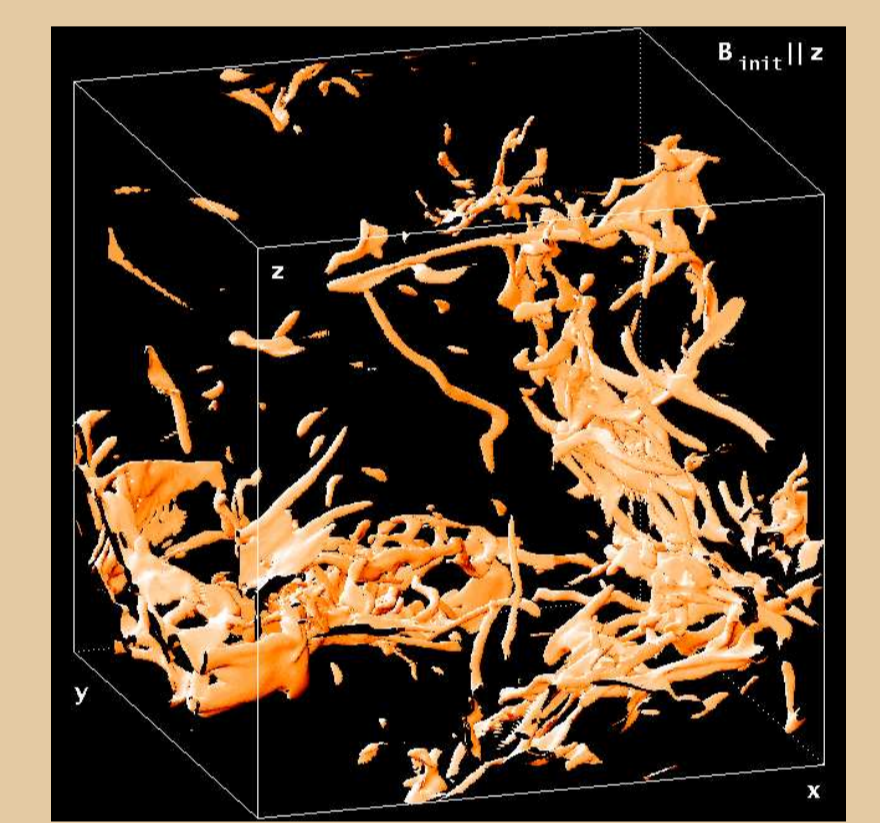


$\Delta$ -variance plots for the three maps shown above.

Radiative transfer effects change the spectral index typically by up to 0.3. The direction and strength of the change mainly depends on the velocity structure. Extinction maps can circumvent this problem, but lack velocity information.

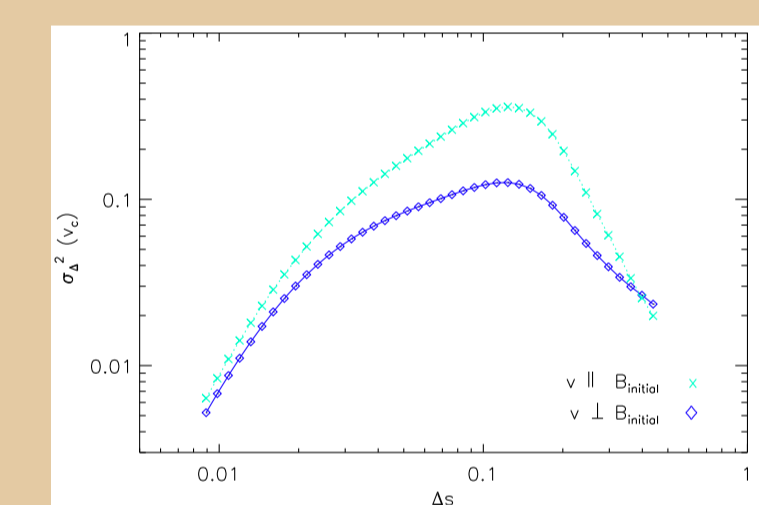
## Magnetic fields

Strong magnetic fields produce significant changes in the structure produced by interstellar turbulence.



Iso-density surfaces in a magneto-hydrodynamic model with an initially homogeneous magnetic field in  $z$ -direction with  $B^2/\mu_0 = 10\rho c_s^2$ .

Dynamically important magnetic fields impose a preferred direction on the turbulent structures.



$\Delta$ -variance plots of the velocity components in  $x$  and  $z$ -direction.

Motions perpendicular to the initial field are strongly suppressed. Strong fields retain their initial direction in large parts of the cloud leading to a global anisotropy.

## Conclusions

**Only large-scale driven turbulence shows the observed  $\Delta$ -variance behaviour.** Decaying turbulence at evolved stages and smaller-scale driven turbulence cannot reproduce the observed scaling relations.

The observed steepening of the  $\Delta$ -variance at small scales resembles the effect of numerical dissipation in the models. A physical mechanism providing dissipation at that scale could be ambipolar diffusion (Zweibel & Josafatsson 1983), which indeed acts at scales of order 0.04 pc for typical molecular cloud conditions (Klessen 2000). **The observed steepening may be the first observational evidence of the viscous dissipation scale in molecular cloud turbulence**

## References

Bensch F. et al. 2001, *A&A* 366, 636  
 Falgarone E. et al. 1998, *A&A* 331, 669  
 Goodman A.A. et al. 1998, *ApJ* 504, 223  
 Klessen R.S. 2000, *ApJ* 535, 869  
 Heithausen A., Thaddeus P. 1990, *ApJ* 353, L49  
 Mac Low M.-M., Ossenkopf V. 2000, *A&A* 353, 339  
 Mac Low et al. 1998, *Phys.Rev.Lett.* 80, 2754  
 Ossenkopf V. et al. 2000, in: Gurzadyan V.G., Ruffini R. (eds.), *The Chaotic Universe*, p. 394  
 Stone, J. M., & Norman, M. L. 1992, *ApJS* 80, 753 and 791  
 Stutzki J. et al. 1998, *A&A* 336, 697  
 Vázquez-Semadeni E. et al. 1997, *ApJ* 474, 292  
 Zweibel E.G., Josafatsson K. 1983, *ApJ* 270, 511